Analysis of repeated liquefaction behavior in shaking table test and triaxial test using energy approach

Jirat Teparaksa[1] and J. Koseki[2]

[1] Strategia Engineering Consultant Co., Ltd., Bangkok, 10400, Thailand, Formerly Department of Civil Engineering, The University of Tokyo, Tokyo, 113-8656, Japan.
[2] Department of Civil Engineering, The University of Tokyo, Tokyo, 113-8656, Japan.

ABSTRACT

Throughout the reports from many countries, it is well-known that soil liquefaction can occur repeatedly at the same spot even though excess pore water pressure was fully dissipated and process of reconsolidation together with soil aging were taken place. In most cases, the second liquefaction generally causes more severe damage compared to the first one. There are evidences supporting that induced strain amplitude during liquefaction significantly affects the next liquefaction resistance. In order to study more in the detail, this paper presents investigation of repeated liquefaction behavior of fine silica sand in shaking table and triaxial apparatuses using energy approach.

Keywords: 1-g shaking table; triaxial; energy; repeated liquefaction

1 INTRODUCTION

The most recent re-liquefaction event in Japan (Wakamatsu, 2012) and New Zealand (Cubrinovski et al., 2012) have raised concern to many practicing engineers and researchers. Repeated liquefaction can occur not only during immediate aftershock but also over the period of time where excess pore water pressure had been dissipated and process of reconsolidation was taken place. In addition, it was observed that second liquefaction normally caused more severe damage than the first one.

It was then discovered that not only stress amplitude but also strain amplitude play an important role in the next liquefaction resistance. Wahyudi et al. (2015) and Teparaksa and Koseki (2016) showed results from a series of re-liquefaction test with various different strain amplitudes. It was concluded that when specimen is sheared at low strain amplitude, the resistance against the next liquefaction highly increases. Moreover, Teparaksa and Koseki (2018) presented that the behavior of post-heavily-liquefied soil is far different from the intact.

During liquefaction, dissipated energy is accumulated which can be divided into two components using Phase Transformation Line (PTL) where soil behavior changes from contraction to dilation (Ishihara and Okada, 1978; 1982). Wahyudi and Koseki (2015) separated dissipated energy into two components so-called positive impact and negative impact. The former is the energy accumulated before the stress path crossed PTL which promotes an increase in the next liquefaction resistance while the latter is dissipated energy after crossing PTL causing reduction in the subsequent liquefaction resistance. In their works, the agreement in positive and negative impact was also drawn for the repeated liquefaction in the stack-ring shear apparatus. In order to verify the method of dissipated energy and to compare the result of two apparatuses, repeated liquefaction tests were carried out in shaking table and triaxial apparatus.

2 MATERIAL AND APPARATUS

Silica sand with number seven grading was employed for both shaking table and triaxial tests. It has a specific gravity of 2.640, the maximum void ratio of 1.243, and the minimum void ratio of 0.743. Its gradation curve is compared with that of Toyoura Sand in Fig. 1.

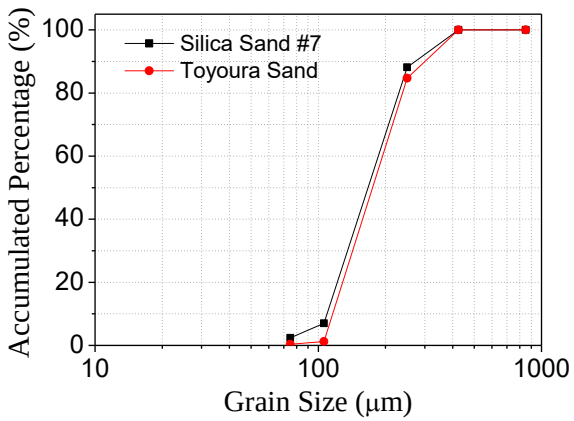

Fig. 1. Gradation of the Silica sand

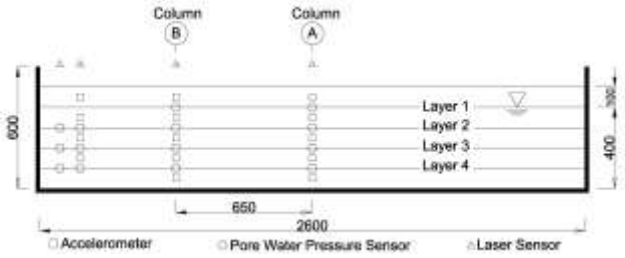

Fig. 2. Sensor location in soil models (unit in mm.)

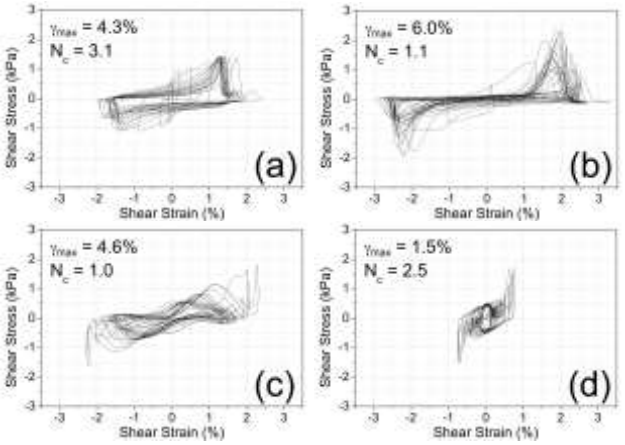

Fig. 3. Relationship of shear stress and shear strain computed from acceleration at layer 2 (-20cm) in (a) 1st shake, (b) 2nd shake, (c) 3rd shake and (d) 4th shake (T7, 300 gal)

3 APPARATUSES AND TESTING PROGRAM

3.1 Shaking Table Apparatus

Five sand levels of 10-cm thick were prepared by air-pluviation method in a soil container with dimensions of 2600 x 400 mm (in plan) x 600 mm high. Saturation was done by filling water through pipes installed at the bottom of soil container to the level of 40 cm height. The top 10 cm was unsaturated. Piezometer attached to the container was used to confirm the level of ground water.

Each ground model was instrumented with 14 uniaxial accelerometers, 14 power water pressure transducers and 4 laser sensors as illustrated in Fig. 2. Accelerometers at different levels were employed to record ground motions during liquefaction test which later were used for stress and strain calculation (Koga and Matsuo, 1990). Laser sensors installed at the top of ground surface to monitor surface settlement to compute the relative density.

Testing program started with different low accelerations ranging from 200, 300 and 400 gal. During repeated liquefaction test, if Double Amplitude shear strain (γ_{DA}) exceeded 1.5%, the same level of acceleration is applied in the next liquefaction stage. On the other hand, if the γ_{DA} is lower than 1.5%, input acceleration is increased by 100 gal in the subsequent stage. The test continued until 1000 gal which is the capacity of shaking table. Liquefaction resistance in terms of number of cycle is calculated at γ_{DA} =1.5%.

3.2 Triaxial Apparatus

Cylindrical specimens of 75 mm diameter and 150 mm height were also prepared by air-pluviation method to reach initial relative density of approximately 50%. Specimen saturation was performed by double vacuum method (Ampadu and Tatsuoka, 1993). Consequently, Skempton's B-value became over 0.95. It is noted that counter weight balance of loading piston was employed to avoid disturbance to the specimen during preparation.

Specimen was then consolidated from confining pressure of 30 kPa to that of 100 kPa. Pressure increasing rate was kept small at 5 kPa/min to maintain deviatoric stress at 0 kPa by controlling simultaneously the axial loading system. Consolidation time was 15 minutes before starting liquefaction test.

Repeated liquefaction tests were carried out with Cyclic Stress Ratios (CSR) of 0.11. By applying loading under undrained condition, excess pore water pressure is generated accompanied by axial strain (ε_a) accumulation. Each test was subjected to different ε_a histories ranging from 1%, 2%, 5%, 7% and 10%. Once, a specific amount of Double Amplitude axial strain ($\varepsilon_{a,DA}$) is reached the loading stops and the left over strain is adjusted back to zero which normally corresponds with zero effective stress. After that excess pore water pressure was released through drainage valve allowing reconsolidation process back to initial confining pressure of 100 kPa. Besides, cyclic loading was terminated at extension side to unify possible effect of induced anisotropy. Then, the next liquefaction stage was continued. It is noted that, to be corresponding with shaking table test, number of cycle was calculated at $\varepsilon_{a,DA}$=1%. More detail regarding triaxial test was discussed in Teparaksa and Koseki (2017).

4 TEST RESULTS

4.1 Shaking Table Tests

Repeated liquefaction tests were performed on three different ground models with various initial input acceleration (200, 300 and 400 gal). The examples of stress-strain relationship of the first four shakes of layer 2 (as defined in Fig. 2.) subjecting to constant 300 gal acceleration is presented in Fig. 3. The number of cycle (Nc) to reach γ_{DA} =1.5% together with the maximum strain amplitude ($\gamma_{DA,max}$) are also shown in the figure. $\gamma_{DA,max}$ was 4.3% in the first shake and increased to 6.0% followed by gradual decrease in the third and fourth shake. It is opposite to the number of cycle where it was 3.1 cycles in the first shake followed by a decrease to 1 cycle in the third shake. The number of cycle started to increase in the fourth shake. The result can be summarized into relationship between number of cycle, strain amplitude and shaking stage as Fig. 4. It can be seen that when the current shear strain amplitude was more than that in the previous stage, liquefaction resistance in the next stage decrease and vice versa.

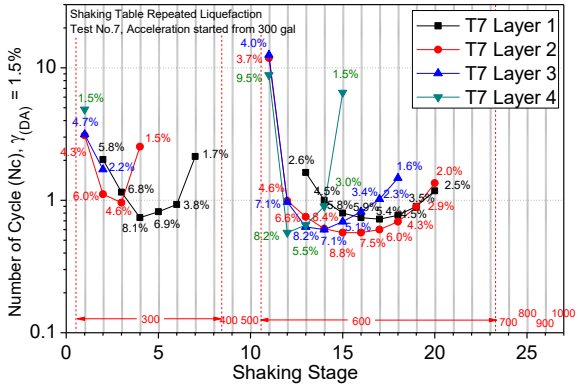

Fig. 4. Liquefaction resistance in shaking table test.

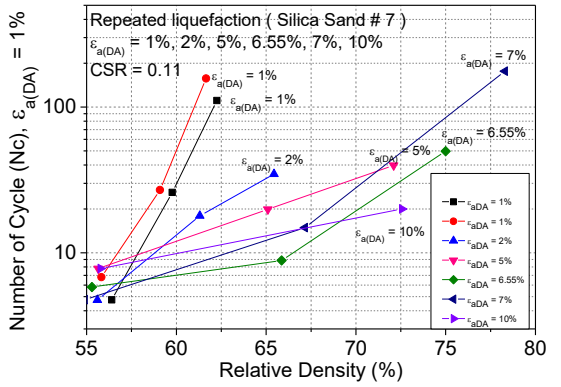

Fig. 5. Relationship between number of cycles to cause liquefaction (i.e. DA axial strain = 1%) and relative density.

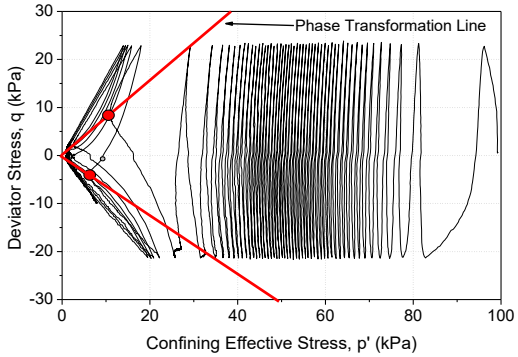

Fig. 6. Phase transformation line in traxial liquefaction test.

4.2 Triaxial Tests

Repeated liquefaction tests were carried out with various strain amplitude from 1% to 10%. The results is summarized in terms of number of cycle to reach $\varepsilon_{a,DA}$=1% and relative density as illustrated in Fig. 5. It can be seen that at the second and third liquefaction stage, though specimens with 1% and 2% strain history induced smaller change in relative density compared to the other, their liquefaction resistance are much higher.

5 ENERGY ANALYSIS

During liquefaction, dissipated energy (ΔW) is accumulated which can be calculated from the hysteretic loop of stress and strain relationship as can be defined in equation 1.

$$\Delta W = \int q d\varepsilon_a , \Delta W = \int \tau d\gamma \quad (1)$$

Where q is deviatoric stress, ε_a is axial strain, τ is shear stress and γ is shear strain. Ishihara and Okada (1978, 1982) proposed a virtual line called as PTL in effective stress path to separate liquefaction behavior as shown in Fig. 6. Soil behavior before the effective stress path touches PTL is contractive. After that, behavior changes to dilative. Regarding this finding, Wahyudi et al. (2015) suggested that ΔW can also be divided into two types using PTL. During contractive behavior, ΔW (hereinafter called as "positive impact, PI") affects the next liquefaction resistance positively. In contrast, ΔW after passing PTL (hereinafter called as "negative impact, NI") reduces future liquefaction resistance.

Occastionally, effective stress path did not pass through the origin due to possible several reasons such as interlocking effect or errors in stress monitoring. Thus, stress correction factor was applied following Koseki et al. (2005 together with effect of membrane force for triaxial test results (Henkel and Gilbert, 1952).

Due to the difference in confining pressure between triaxial test and shaking table test, ΔW was modified by taken confining pressure into the account (hereinafter named as normalized dissipated energy, ΔW') which can be expressed as equation 2.

$$\Delta W' = \int \frac{q}{p'} d\varepsilon_a , \Delta W' = \int \frac{\tau}{p'} d\gamma \quad (2)$$

where p' is effective confining stress. Relationship between ΔW' and accumulated axial strain corresponding with Fig. 6 is shown in Fig. 7. During contractive behavior, ΔW' accumulated at almost constant rate. After passing PTL, rate of accumulation changed rapidly. ΔW' was then separated into PI and NI. Both PI and NI which were generated in the immediate-past-stage are used to plot relation with the current liquefaction resistance in terms of number of cycle as shown in the Fig. 8. for triaxial test. It is clear that there is unique trend of weak (Nc =0-20 cycles), moderate (Nc=21-50 cycles), strong (Nc>50 cycles) specimen regardless of liquefaction stage and density.

For shaking table test result, ΔW' can also be computed and compared with triaxial test result since this method takes confining pressure into the account. However, in shaking table, CSR cannot be controlled and is not constant during the shaking test, using number of cycle as liquefaction resistance may not be appropriate. Thus, the cyclic resistance in the next stage was presented by means of CSR_{eq20} which is equivalent CSR that causes γ_{DA}=1.5% at 20 cycles based on cumulative damage concept (Tatsuoka et al., 1986). The relationship between PI, NI and the next liquefaction resistance is shown in Fig. 9.

In order to compare result of triaxial and shaking table test, number of cycle in triaxial test was converted into CSR_{eq20}. The comparison is presented in Fig. 10.

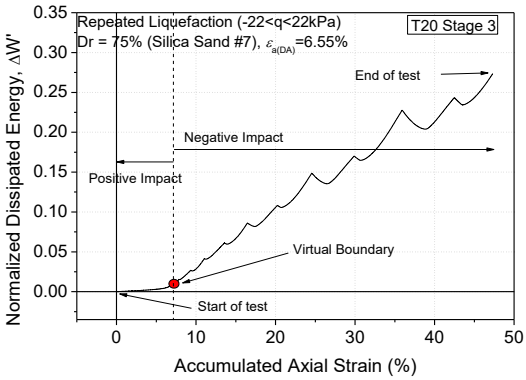

Fig. 7. Relationship of normalized dissipated energy and accumulated axial strain

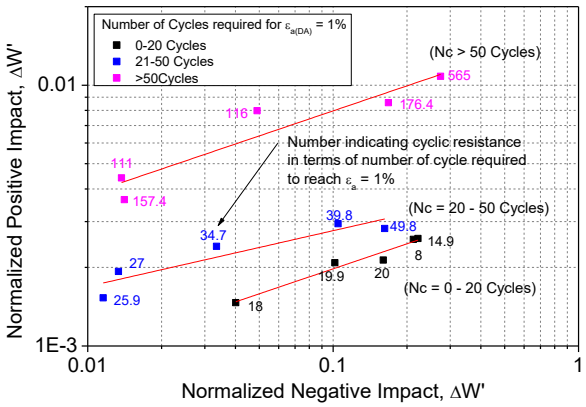

Fig. 8. Relationship between positive impact and negative impact of the previous liquefaction stage to next cyclic resistance in triaxial test

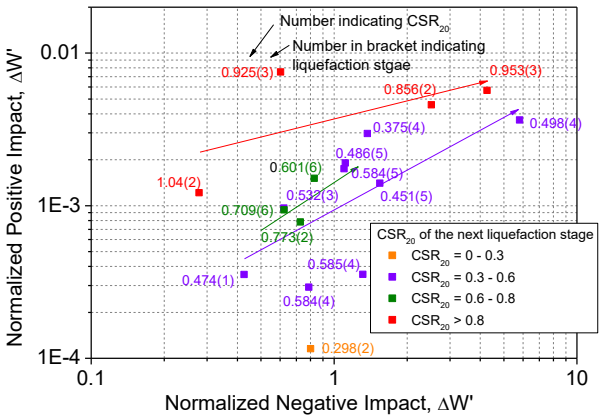

Fig. 9. Relationship of positive impact and negative impact generated in previous liquefaction stage to cyclic stress ratio at 20 cycles of the next liquefaction stage in shaking table test.

It can be seen that CSR_{eq20} of triaxial was much lower than that of shaking table test for similar values of normalized positive and negative impacts indicating inconsistance of the compariosn.

5 CONCLUSION

Energy approach was employed to analyze liquefaction behavior of fine silica sand in a series of shaking table and triaxial test. It was found that

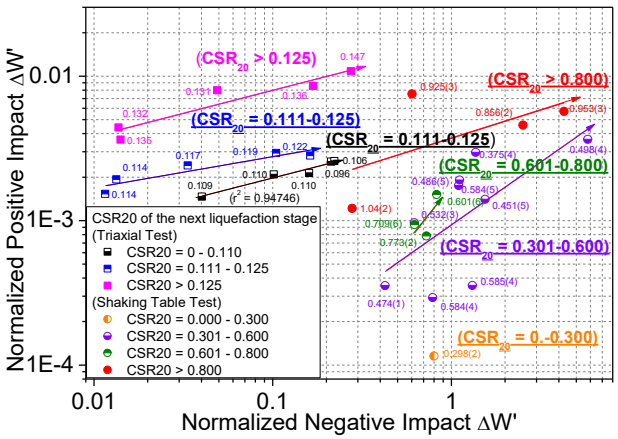

Fig. 10. Relationship between positive impact and negative impact to the next liquefaction resistance in term of CSR which caused liquefaction at 20 cycles

liquefaction resistance in terms of CSR_{eq20} of shaking table was higher than that of triaxial at similar values of normalized PI and NI. One of possible major reasons is degree of saturation. In triaxial, saturation was done by double vacuum method while in shaking table was water filling.

REFERENCES

Ampadu, S.K. and Tatsuoka, F. (1993). Effect of setting method on the behavior of clays in triaxial compression from saturation to undrained shear. Soils and Foundations. 33(2). 14-34.

Henkel, D. and Gilbert, G. (1952). The effect measured of the rubber membrane on the triaxial compression strength of clay samples. Geotechnique, 3(1), 20-29.

Ishihara, K. and Okada, S. (1978). Effects of stress history on cyclic behavior of sand. Soils and Foundations, 18(4), 31-45.

Ishihara, K. and Okada, S. (1982). Effects of large pre-shearing on cyclic behavior of sand. Soils and Foundations, 22(3), 109-125.

Koga, Y. and Matsuo, O. (1990). Shaking table tests of embankments resting on liquefiable sandy ground. Soils and Foundations, 30(4), 162-174.

Koseki, J., Yoshida, T. and Sato T. (2005). Liquefaction properties of Toyoura sand in cyclic torsional shear tests under low confining stress. Soils and Foundations, 45(5), 103-113.

Tatsuoka, F., Maeda, S., Ochi, K. and Fujii, S. (1986). Prediction of cyclic undrained strength of sand subjected to irregular loadings. Soils and Foundations, 26(2). 73-90.

Teparaksa J. and Koseki J. (2016). Behaviour of silica sand under repeated liquefaction using triaxial apparatus. Proc., the 18th International Symposium, Japanese Society of Civil Engineers. 67-68.

Teparaksa J. and Koseki J. (2017). Silica sand behavior under repeated liquefaction in cyclic triaxial test. Proc., the 19th International Conference on Soil Mechanics and Geotechnical Engineering, Seoul. 1593-1596.

Teparaksa K. and Koseki K. (2018). Effect of past history on liquefaction resistance of level ground in shaking table test. Geotechnique Letters. 8(4). 1-6

Wahyudi S., Koseki J., Sato T. and Chiaro G. (2015). Multiple-liquefaction behavior of sand in cyclic simple stacked-ring shear tests. International Journal of Geomechanics, 16(5), C4015001.